Higher Excited Electronic Transitions of Polyacetylene Cations $HC_{2n}H^+$ $n = 2-7$ in Neon Matrixes

Jan Fulara,[†,‡] Michel Grutter,[†] and John P. Maier*[,†]

Department of Chemistry, University of Basel, Klingelbergstrasse 80, CH-4056 Basel, Switzerland, and Institute of Physics, Polish Academy of Sciences, Al. Lotników 32-46, Pl-02668 Warsaw, Poland

Received: July 24, 2007; In Final Form: September 5, 2007

The polyacetylene $HC_{2n}H^+$ $n = 2-7$ cations were produced from a mixture of diacetylene with helium in a hot cathode-discharge source. After a mass−selective deposition, their absorption spectra were studied in 6 K neon matrixes. Besides the known $\tilde{A}^2\Pi \leftarrow \tilde{X}^2\Pi$ system, several new transitions to higher excited $^2\Pi$ electronic states of these cations have been observed. In the case of HC_4H^+ and HC_6H^+, only one new weak absorption system has been detected with the onset at 336.1 and 417.2 nm, respectively. These $\tilde{C}^2\Pi \leftarrow \tilde{X}^2\Pi$ transitions form a series that extends to $HC_{10}H^+$. Two further electronic transitions are observed for HC_8H^+ through to $HC_{14}H^+$; a weaker $\tilde{B}^2\Pi_u \leftarrow \tilde{X}^2\Pi_g$ and a strong $\tilde{E}^2\Pi_u \leftarrow \tilde{X}^2\Pi_g$ in the UV. The integrated intensity of the UV system of the polyacetylene cations exceeds that of the $\tilde{A}^2\Pi \leftarrow \tilde{X}^2\Pi$ transition by an order of magnitude.

Introduction

Polyacetylene cations $HC_{2n}H^+$ are model compounds for open-shell carbon chain radicals. HC_4H^+ was the first largest organic cation that was observed as a mysterious "T"-emission[1] in the electrical discharges running through organic vapors. Later, it was analyzed and assigned to the $\tilde{A}^2\Pi_u \leftarrow \tilde{X}^2\Pi_g$ transition of HC_4H^+.[2] The $HC_{2n}H^+$ $n = 3, 4$ cations also decay radiatively from the $\tilde{A}^2\Pi$ state, though with smaller quantum yields.[3]

The fluorescence of $HC_{2n}H^+$ $n = 2-4$ induced by electron impact of the neutral parent has been studied in effusive[3] and supersonic beams.[4,5] Also, laser-induced fluorescence (LIF) was used for the spectroscopy of these cations.[5−7] The geometric structure of HC_4H^+ could be determined from the rotationally resolved LIF spectra of several isotopomers.[6] The $\tilde{A}^2\Pi \leftarrow \tilde{X}^2\Pi$ electronic transition of $HC_{2n}H^+$ $n = 3-5$ has been investigated in the gas phase by absorption methods: cavity ring down[8−10] and laser frequency modulation.[9,11] In the case of $n = 3, 4$, the origin band was rotationally resolved.[8,9,11]

The polyacetylene cations $HC_{2n}H^+$ $n = 2-4$ were also studied in rare gas matrixes in emission[7,12] and $n = 2-8$ by absorption spectroscopy.[13] Recently, their transitions were observed in the gas phase on collisionally cooled ions in a RF trap and using a two color excitation-dissociation scheme.[14]

All of the above works concern the lowest $\tilde{A}^2\Pi$ and $\tilde{X}^2\Pi$ states of polyacetylene cations. Little is known about their higher excited electronic states. Some spectroscopic data come from photoelectron studies of the smaller polyacetylenes ($n = 2-4$).[15,16] Higher excited electronic states were studied by theoretical methods but were restricted to the smallest cations ($n = 2, 3$).[17−19] In this contribution, the electronic absorption spectra that involve the excitation to the higher ($\tilde{E}$...$\tilde{B}$)$^2\Pi$ electronic states of $HC_{2n}H^+$ $n = 2-7$ in 6 K neon matrixes are reported.

Experimental Section

Details of the apparatus for the matrix isolation of mass-selected molecular ions has been given.[13] Polyacetylene cations $HC_{2n}H^+$ ($n = 2-7$) were produced in a hot cathode-discharge ion source from diacetylene diluted with helium in the ratio 1:5 to 1:1, with a higher concentration being required for the largest species. Cations were extracted from the source, deflected by 90°, and selected with a quadrupole mass filter. Ions of a given m/e were co-deposited with neon during 2 h on a rhodium-coated sapphire substrate held at 6 K. After the matrix growth, the absorption spectrum was measured in the 220−1100 nm region by passing monochromatized light from a xenon arc or halogen lamp through the matrix parallel to the substrate surface. A photomultiplier or silicon diode was used to detect the photons. Photobleaching experiments were carried out by exposing the matrix surface to a medium-pressure mercury lamp equipped with a cutoff filter ($\lambda > 295$ nm) to identify the absorptions of charged species.

Results and Discussion

Short-Wavelength Transitions of $HC_{2n}H^+$ $n = 2-4$. The spectra measured after mass-selected co-deposition of polyacetylene cations with neon exhibit their known $\tilde{A}^2\Pi \leftarrow \tilde{X}^2\Pi$ electronic transitions.[7,13] If the kinetic energy of deposited cations was >50 eV, then absorptions of neutral $C_{2n}H$ fragments were also observed in the matrix.[20] Apart from the bands of polyacetylene cations, and sometimes the bands of $C_{2n}H$, several much weaker absorption bands are also seen, which are located at a shorter wavelength of the $\tilde{A}^2\Pi \leftarrow \tilde{X}^2\Pi$ transition. The weak absorptions decreased in intensity upon UV irradiation similar to the bands of polyacetylene cations. Therefore, they most likely belong to charged species.

Because of the low mass resolution (about ±2 amu) used in the standard depositions, one can presume that the bands are

* To whom correspondence should be addressed. E-mail: J.P.Maier@unibas.ch.
† University of Basel.
‡ Polish Academy of Sciences.

10.1021/jp075807t CCC: $37.00 © 2007 American Chemical Society
Published on Web 10/30/2007

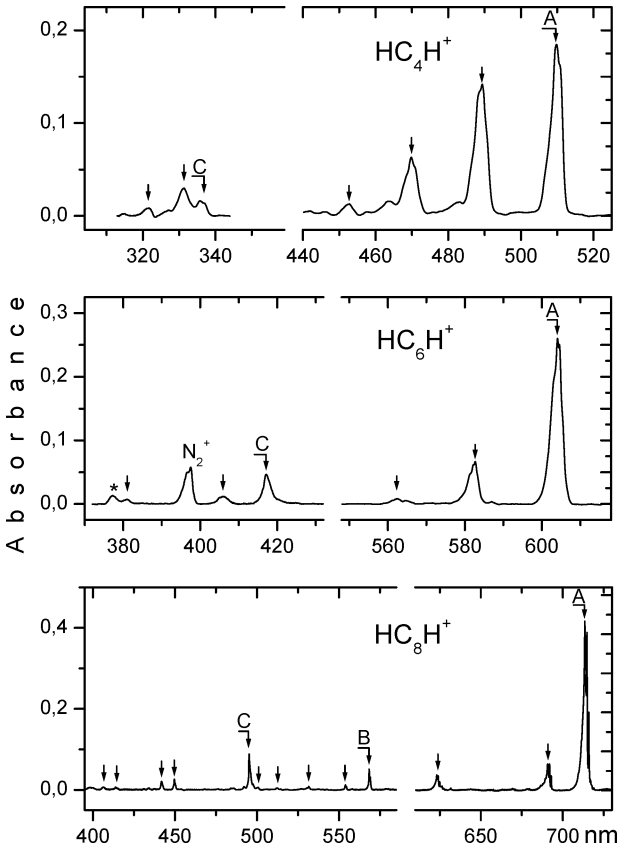

Figure 1. Short-wavelength electronic absorption spectra of di-, tri-, and tetraacetylene cations in 6 K neon matrices. Known $\tilde{A}^2\Pi \leftarrow \tilde{X}^2\Pi$ transitions of these cations[13] are also plotted on the same absorbance scale for intensity comparison. Arrows with horizontal bars mark the origin bands and the capital letter over bars labels the upper electronic state. The N_2^+ band seen in the spectrum of HC_6H^+ is a vacuum impurity. The band marked with star belongs to $H_2C_6H^+$.

due to the cations ($C_{2n}H_m^+$) $m = 1-4$. Recently, the shorter members $C_{2n}H_m^+$ ($n = 2-4$, $m = 1-4$) have been deposited with nearly 1 amu resolution and their electronic spectra have been recorded.[21−24] The experimental conditions were optimized for high ion current. Only the bands of C_6H^+ and C_8H^+ were identified in some old spectra of triacetylene and tetraacetylene cations in neon matrixes in the case when the bands of neutral C_6H and C_8H were also present and the kinetic energy during deposition was higher than 50 eV. Though the electronic spectra of $C_{2n}H_m^+$ ($n = 2-4$, $m = 1-4$) are already known,[22−24] the weak absorption bands that accompany the strong $\tilde{A}^2\Pi \leftarrow \tilde{X}^2\Pi$ electronic transition of $HC_{2n}H^+$ $n = 2-4$ remained unidentified. It is likely that the bands belong to new electronic transition of the polyacetylene cations.

To verify this hypothesis, several depositions of polyacetylene cations of a given *m*/*e* have been performed under conditions when, for example, concentration of diacetylene in the mixture used, pressure in the source, kinetic energy of deposited ions, or mass resolution have been varied. The relative intensities of these weak bands, scaled to the intensity of the origin band of the $\tilde{A}^2\Pi \leftarrow \tilde{X}^2\Pi$ transition of $HC_{2n}H^+$ ($n = 2-4$), remained constant in all the experiments. Hence, the weak absorption bands belong to the new electronic transition of polyacetylene cations.

The best-quality spectra of $HC_{2n}H^+$ $n = 2-4$ obtained are presented in Figure 1. The bands of the $\tilde{A}^2\Pi \leftarrow \tilde{X}^2\Pi$ electronic transition are also shown for comparison of their intensities with those of the weak bands. The shorter-wavelength electronic transition is an order of magnitude weaker than that for the $\tilde{A}^2\Pi \leftarrow \tilde{X}^2\Pi$ system.

The position of the origin band of the second electronic transitions HC_6H^+ at 417.2 nm is shifted ~80 nm toward longer wavelength in comparison with HC_4H^+ (336.1 nm). If this regularity also occurs in the case of HC_8H^+, then the origin band of the second electronic transition is expected around 497 nm. Indeed, a distinct band at 495.2 nm is present in the spectrum of HC_8H^+ (bottom panel of Figure 1). However, a further equally intense band at 568.5 nm is apparent. The shape of the latter differs from the bands of the $\tilde{A}^2\Pi_u \leftarrow \tilde{X}^2\Pi_g$ transition. The intensity ratio of this band to the origin of the $\tilde{A}^2\Pi_u \leftarrow \tilde{X}^2\Pi_g$ transitions was the same in all of the spectra recorded under different conditions. Therefore, the band at 568.5 nm belongs to HC_8H^+ and is the onset of the new $\tilde{B}^2\Pi_u \leftarrow \tilde{X}^2\Pi_g$ electronic transition of this cation.

The band at 495.2 nm lies 2604 cm^{-1} above the origin at 568.5 nm. This energy does not match any vibration of HC_8H^+. It is too small for ν_1 and too large for the ν_2 mode of tetraacetylene cation. DFT frequencies of these modes in the ground state of HC_8H^+ are 3409 and 2205 cm^{-1}. Furthermore, the intensity of the 495.2 nm peak in comparison with the origin band at 568.5 nm precludes that the former can be assigned to any combination band. Hence, the peak at 495.2 (marked with letter C in Figure 1) is assigned to the next, energetically higher lying, electronic transition of HC_8H^+. Weak absorptions, which are seen to the short-wavelength side of each origin band, are the totally symmetric vibrations and their combinations are active in the $\tilde{B}$ and $\tilde{C}$ excited electronic states of HC_8H^+.

As was discussed above, the 495.2 nm origin band of the $\tilde{C}^2\Pi_u \leftarrow \tilde{X}^2\Pi_g$ transition of HC_8H^+ correlates with the origin band of HC_6H^+ and HC_4H^+ at 417.2 and 336.1 nm, respectively. Though no other electronic transition has been detected for di- and triacetylene cations that lies between the weak absorption shown in Figure 1 and the strong $\tilde{A}^2\Pi \leftarrow \tilde{X}^2\Pi$ system, it is assigned as the excitation to the $\tilde{C}$ state to be consistent with the spectrum of HC_8H^+. The position of new origin and vibrational bands of $HC_{2n}H^+$ $n = 2-4$ with their assignments are given in Table 1. This is based on calculated frequencies of normal modes in the ground state of these cations and assuming that they do not differ very much from the observed ones. A high-intensity ratio of the origin band to the vibrational bands justifies this assumption. The frequencies of normal modes were calculated using density functional theory (DFT) with the Becke three parameter Lee−Yang−Parr (B3LYP) exchange correlation functional[25,26] and cc-pVTZ basis set.[27] These were carried out with the Gaussian 03 program package. Calculated frequencies of the totally symmetric modes of polyacetylene cations are included in Table 1.

Doublet and quartet excited electronic states of polyacetylene cations have been studied by theoretical methods.[17−19,28] The energetically lowest-lying $\tilde{a}^4\Pi$ quartet state of di- and triacetylene cations predicted by restricted coupled cluster (RCCSD(T)) method is located above the $\tilde{A}^2\Pi$ state.[19] The transition from the ground state is spin forbidden. Higher excited doublet states of HC_4H^+ have been treated by a semiquantitative and ab initio CI method to explain the weak UV absorption bands observed in an argon matrix.[17] The position of these weak bands agrees well with the present studies; however, the stronger short-wavelength UV band (around 276 nm) reported in ref 17 was not observed. Theoretical calculations for this cation predicted several excited doublet states of $^2\Pi_u$ and $^2\Phi_u$ symmetry.[17] The well-known strong visible band system of HC_4H^+ corresponds to the excitation to the $\tilde{A}^2\Pi_u$ state. Next, the $(2)^2\Pi_u$ state was

TABLE 1: Positions of the Band Maxima (±0.2 nm) Observed for the Higher Electronic Transitions of Polyacetylene Cations ($HC_{2n}H^+$ $n = 2-7$) in 6 K Neon Matrixes and the Suggested Assignments

species	λ/nm	$\tilde{\nu}$/cm^{-1}	$\Delta\tilde{\nu}$/cm^{-1}	assignment[a,b]	
HC_4H^+	336.1	29753	0	0_0^0	$\tilde{C}^2\Pi_u \leftarrow \tilde{X}^2\Pi_g$
	331.0	30211	459	$2\nu_9$	
	321.4	31114	1362	$2\nu_6$	
HC_6H^+	417.2	23969	0	0_0^0	$\tilde{C}^2\Pi_g \leftarrow \tilde{X}^2\Pi_u$
	406.0	24631	662	ν_4	
	381.0	26247	2278	ν_2	
HC_8H^+	568.5	17590	0	0_0^0	$\tilde{B}^2\Pi_u \leftarrow \tilde{X}^2\Pi_g$
	553.9	18054	464	ν_5	
	531.7	18808	1218	ν_4	
	512.4	19516	1926	ν_3	
	500.7	19972	2382	$\nu_3 + \nu_4$	
	495.2	20194	0	0_0^0	$\tilde{C}^2\Pi_u \leftarrow \tilde{X}^2\Pi_g$
	449.6	22242	2048	ν_3	
	441.8	22635	2441	$\nu_3 + \nu_4$	
	413.8	24166	3972	$2\nu_3$	
	406.3	24612	4418	$2\nu_3 + 2\nu_4$	
	242.4	41254	0	0_0^0	$\tilde{E}^2\Pi_u \leftarrow \tilde{X}^2\Pi_g$
	231.0	43290	2036	ν_3	
$HC_{10}H^+$	649.2	15404	0	0_0^0	$\tilde{B}^2\Pi_g \leftarrow \tilde{X}^2\Pi_u$
	575.0	17391	1987	ν_4	
	567.3	17627	0	0_0^0	$\tilde{C}^2\Pi_g \leftarrow \tilde{X}^2\Pi_u$
	506.1	19759	2132	ν_3	
	497.0	20121	2494	$\nu_3 + \nu_6$	
	489.4	20433	2806	$\nu_3 + 2\nu_6$	
	275.6	36284	0	0_0^0	$\tilde{E}^2\Pi_g \leftarrow \tilde{X}^2\Pi_u$
	261.4	38256	1972	ν_4	
$HC_{12}H^+$	729.5	13708		0_0^0	$\tilde{B}^2\Pi_u \leftarrow \tilde{X}^2\Pi_g$
	637.1	15696	1988	ν_4	
	632.8	15803	2095	ν_3	
	562.2	17787	4079	$\nu_3 + \nu_4$	
	559.9	17860	4152	$2\nu_3$	
	538.5	18570	0	0_0^0	$\tilde{D}^2\Pi_u \leftarrow \tilde{X}^2\Pi_g$
	308.8	32382	0	0_0^0	$\tilde{E}^2\Pi_u \leftarrow \tilde{X}^2\Pi_g$
	290.0	34483	2101	ν_3 or ν_4	
$HC_{14}H^+$	803.4	12447	0	0_0^0	$\tilde{B}^2\Pi_g \leftarrow \tilde{X}^2\Pi_u$
	696.9	14349	1902	ν_5 or ν_4	
	609.8	16399	0	0_0^0	$\tilde{D}^2\Pi_g \leftarrow \tilde{X}^2\Pi_u$
	342.3	29214	0	0_0^0	$\tilde{E}^2\Pi_g \leftarrow \tilde{X}^2\Pi_u$
	321.6	31095	1881	ν_5 or ν_4	

[a] The B, C... labels of electronic states are not an absolute numbering. [b] The assignment of the vibrational modes uses the ground-state numbering and assumes that the frequencies in the excited states of $HC_{2n}H^+$ do not differ much from the calculated ones: HC_4H^+ (all vibrations): (σ_g: $\nu_1 = 3368$, $\nu_2 = 2249$,$\nu_3 = 958$); (σ_u: $\nu_4 = 3362$, $\nu_5 = 1920$); (π_g: $\nu_6 = 776/664$, $\nu_7 = 508/484$); (π_u: $\nu_8 = 777/667$, $\nu_9 = 218/212$); only σ_g modes for the larger species: HC_6H^+ (σ_g): $\nu_1 = 3393$, $\nu_2 = 2255$, $\nu_3 = 1985$, $\nu_4 = 656$; HC_8H^+ (σ_g): $\nu_1 = 3409$, $\nu_2 = 2205$, $\nu_3 = 2120$, $\nu_4 = 1411$, $\nu_5 = 500$; $HC_{10}H^+$ (σ_g): $\nu_1 = 3419$, $\nu_2 = 2187$,$\nu_3 = 2144$, $\nu_4 = 2012$, $\nu_5 = 1153$, $\nu_6 = 404$; $HC_{12}H^+$ (σ_g): $\nu_1 = 3426$, $\nu_2 = 2216$,$\nu_3 = 2105$, $\nu_4 = 2083$, $\nu_5 = 1543$, $\nu_6 = 977$, $\nu_6 = 338$; $HC_{14}H^+$ (σ_g): $\nu_1 = 3432$, $\nu_2 = 2219$,$\nu_3 = 2160$, $\nu_4 = 2033$, $\nu_5 = 2013$, $\nu_6 = 1351$, $\nu_7 = 848$, ν_8=291), The frequencies were calculated with DFT employing the B3YLP exchange correlation functional and cc-pVTZ basis set. A high-intensity ratio of the origin band to the vibrational bands points to a small geometry change upon the electronic excitation and justifies the assumption.

predicted at 4.2 eV above the ground state. This energy agrees well with the position of the 0_0^0 band in a neon matrix (3.69 eV). The predicted oscillator strength for this transition is ~3 times smaller than that for the $\tilde{A}^2\Pi_u$ state.

Multireference configuration interaction calculations (MRCI) have been carried out to determine the energy of the doublet electronic states of HC_6H^+.[18] The energy of the $\tilde{A}^2\Pi_g$ state (2.22 eV) reproduces well the position of the 0_0^0 band of HC_6H^+

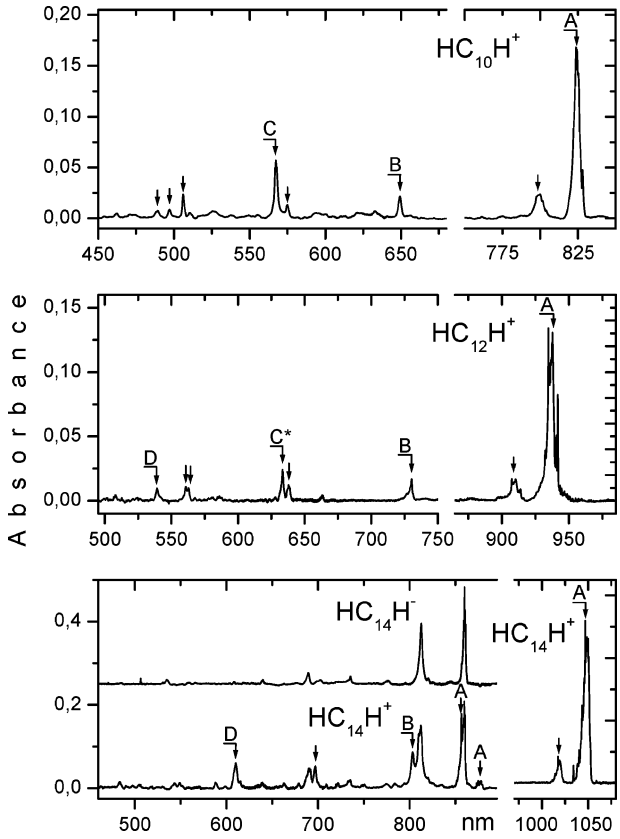

Figure 2. Short-wavelength electronic absorption spectra of polyacetylene cations, $HC_{2n}H^+$ $n = 5-7$, in 6 K neon matrices. Known $\tilde{A}^2\Pi \leftarrow \tilde{X}^2\Pi$ transitions of these cations[13] are also plotted in the same absorbance scale for intensity comparison. Arrows with horizontal bars mark the origin bands, and the capital letter over bars labels the upper electronic state. C* in the spectrum of $HC_{12}H^+$ indicates where the origin of the $\tilde{C}^2\Pi_u \leftarrow \tilde{X}^2\Pi_g$ system is expected. The $\tilde{A}^2\Pi \leftarrow \tilde{X}^2\Pi$ transition of $HC_{14}H^+$ overlaps with the $(2)^2\Pi_u \leftarrow \tilde{X}^2\Pi_g$ absorption of $HC_{14}H^-$,[29] formed in the matrix by electron capture.

(2.05 eV) in the gas phase.[3] The next optically allowed transition (though weaker than the former) is to the $(2)^2\Pi_g$ state, located 3.58 eV above the ground state. The calculated energy of this state is overestimated by ~0.6 eV relative to the present experimental value (2.97 eV). A weaker transition to the (3) $^2\Pi_g$ state is predicted at 4.54 eV. The first excited electronic state of $^2\Sigma_g^+$ symmetry, which results from the $7\sigma_g \rightarrow 2\pi_u$ excitation, is located 7.8 eV above the ground state. No other strong electronic transition has been found below 6 eV for this cation.[18] In the case of HC_8H^+, complete-active-space self-consistent-field (CASSCF) calculations were performed[28] but they were restricted to the lowest $\tilde{A}^2\Pi_u$ excited electronic state. Therefore, the new weak band systems of this cation seen in Figure 1 were assigned, by analogy to smaller polyacetylene cations, to the $\tilde{B}^2\Pi_u \leftarrow \tilde{X}^2\Pi_g$ and $\tilde{C}^2\Pi_u \leftarrow \tilde{X}^2\Pi_g$ transitions. The symmetry of the excited electronic states involved in the optical transitions of $HC_{2n}H^+$ $n = 2-4$ cannot be deduced from the matrix experiments; hence, it is based on the results of the theoretical calculations.

Short-Wavelength Transitions of $HC_{2n}H^+$ $n = 5-7$. A search for a short-wavelength band system of larger polyacetylene cations has been undertaken. Several depositions of $HC_{2n}H^+$ $n = 5-7$ in neon matrixes were carried out and new bands have been found when the kinetic energy of deposited cations did not exceed 50 eV and the mass resolution was ≤2 amu. These are shown in Figure 2. Besides the new absorptions, the known $\tilde{A}^2\Pi \leftarrow \tilde{X}^2\Pi$ bands are also shown for comparison of their intensities. New band systems seen in Figure 2 are likely due

to $HC_{2n}H^+$ $n = 5-7$ because the cations were deposited at low kinetic energy, their fragmentation (e.g., to $C_{2n}H^+$) was suppressed, and their intensities correlated with the bands of the $\tilde{A}^2\Pi \leftarrow \tilde{X}^2\Pi$ transition.

It is known from previous experiments that in order to get strong absorptions of the cations like $C_{2n}H^+$ or $H_2C_{2n}H^+$ ($n = 2-4$) for which higher members can be expected in the present studies as a result of a limited mass resolution, the conditions of the experiments had to be optimized.[23,24] The electronic absorption spectra of $C_{2n}H^+$ or $H_2C_{2n}H^+$ $n = 5-7$ are unknown. However, one can predict the position of the 0_0^0 band of these cations by using the data for smaller cations[23,24] and extrapolating the linear relationship of the wavelength of the 0_0^0 band as a function of the number of carbon atoms. The origin band of the $\tilde{A}^3\Sigma^- \leftarrow \tilde{X}^3\Sigma^-$ transition of $C_{2n}H^+$ is expected at 741, 854, and 966 nm and the band of the $\tilde{B}^1A_1 \leftarrow \tilde{X}^1A_1$ system of $H_2C_{2n}H^+$ at 559, 650, and 741 nm for $n = 5-7$, respectively. Alternatively, the onset of weak bands in Figure 2 lies at 649.2, 729.5, and 803.4 nm for the $HC_{2n}H^+$ $n = 5-7$ selections. Therefore, the $C_{2n}H^+$ cations can be excluded while the absorptions of $H_2C_{2n}H^+$ may interfere to some extent with the bands of the new system. However, they do not overlap with the origin band of the new system shown in Figure 2 for $HC_{2n}H^+$ $n = 5-7$.

The onset of weak absorptions of $HC_{10}H^+$ is bathochromically shifted by ~80 nm compared to the 0_0^0 band of the new $\tilde{B}^2\Pi_u \leftarrow \tilde{X}^2\Pi_g$ transition of HC_8H^+. If such a trend would be continued for the larger $HC_{2n}H^+$ $n = 6$, 7 cations, then their origin is expected around 729 and 809 nm. The bands observed at 729.5 and 803.4 nm are close to this prediction. In the spectrum of $HC_{14}H^+$ (bottom panel in Figure 2), the origin band is obscured by the absorptions of $HC_{14}H^-$. To illustrate this, the electronic absorption spectrum of $HC_{14}H^-$ recorded previously[29] is also plotted. In the present studies, $HC_{14}H^-$ originates from $HC_{14}H^+$, which was neutralized during deposition, and the newly formed neutrals have captured a second electron forming $HC_{14}H^-$. The onset of new weak absorptions of $HC_{2n}H^+$ $n = 5-7$, marked with letter B in Figure 2 ,was assigned to the $\tilde{B}^2\Pi \leftarrow \tilde{X}^2\Pi$ transition by analogy to HC_8H^+.

In the spectrum of $HC_{10}H^+$ (top panel in Figure 2), the band at 567.3, marked with letter C, dominates among other weak new bands. It lies 2223 cm^{-1} above the origin band of the $\tilde{B}^2\Pi_g \leftarrow \tilde{X}^2\Pi_u$ transition and therefore can be assigned to the ν_2 mode, which is active in the $\tilde{B}^2\Pi_g$ state. The ground-state frequency calculated with the same level of theory and basis set as for the smaller $HC_{2n}H^+$ $n = 2-4$ cations (B3LYP/ cc-pVTZ) is 2187 cm^{-1}. The band at 567.3 nm is shifted ~72 nm from the origin of the $\tilde{C}^2\Pi_u \leftarrow \tilde{X}^2\Pi_g$ transition of HC_8H^+. The shift for smaller polyacetylene cations ($HC_{2n}H^+$ $n = 2$, 3) is 81 and 78 nm, respectively. Hence, the peak at 567.3 nm can also be assigned to the origin of the $\tilde{C}^2\Pi_g \leftarrow \tilde{X}^2\Pi_u$ transition of this cation. The intensities in the spectrum of $HC_{10}H^+$ argue in favor of the latter assignment. If the 567.7 nm band involved the ν_2 vibrational excitation, then it would be difficult to explain the intensity pattern around 500 nm in the spectrum of $HC_{10}H^+$.

The electronic spectrum of $HC_{12}H^+$ shown in the middle panel of Figure 2 is quite simple. The origin band at 729.5 nm can be assigned to the $\tilde{B}^2\Pi_u \leftarrow \tilde{X}^2\Pi_g$ electronic transition, similar to what was proposed for HC_8H^+ and $HC_{10}H^+$. The next two moderately intense bands, which are spaced from the origin by 1988 and 2095 cm^{-1}, can be attributed to single excitation of vibrations within the same electronic transition. Their frequencies are characteristic of the C≡C stretching modes of carbon chains. The calculated values of 2083 and 2105 cm^{-1} of the ν_3 and ν_4 modes in the ground state of $HC_{12}H^+$ by the DFT method (B3LYP/cc-pVTZ) are close to these values. The ν_3 and ν_4 modes, which are active in the $\tilde{B}^2\Pi_u$ state of $HC_{12}H^+$, form the combination and overtone bands and are seen in the spectrum around 560 nm. C* marks the position where the origin band of the $\tilde{C}^2\Pi_u \leftarrow \tilde{X}^2\Pi_g$ transition is expected by extrapolation from the smaller polyacetylene cations. Because a regular intensity distribution of the bands in the $\tilde{B}^2\Pi_u \leftarrow \tilde{X}^2\Pi_g$ transition is observed, the former assignment is preferred. The band at 538.5 nm does not fit to the vibrational pattern of the $\tilde{B}^2\Pi_u \leftarrow \tilde{X}^2\Pi_g$ transition. To be consistent with other polyacetylene cations, it was assigned to the origin band of the $\tilde{D}^2\Pi_u \leftarrow \tilde{X}^2\Pi_g$ electronic transition though the $\tilde{C}^2\Pi_u$ state was not observed in this case.

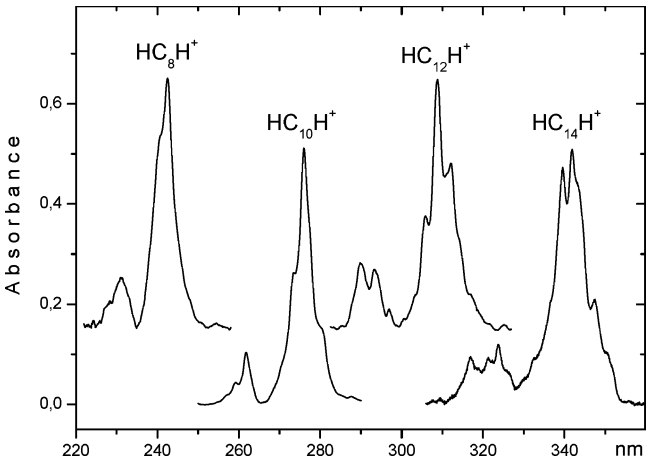

Figure 3. Strong UV $\tilde{E}^2\Pi \leftarrow \tilde{X}^2\Pi$ electronic transition of polyacetylene cations, $HC_{2n}H^+$ $n = 4-7$, in 6 K neon matrices. The intensity of the origin bands is normalized, and a similar peak pattern is apparent.

In the spectrum of $HC_{14}H^+$, bottom panel of Figure 2, three new bands are distinguished: at 803.4, 696.9, and 609.8 nm. The first one is the onset of the $\tilde{B}^2\Pi_g \leftarrow \tilde{X}^2\Pi_u$ transition. The second lies 1902 cm^{-1} above the origin and is assigned to the excitation of the ν_4 or ν_5 mode, which correlate with frequencies in the ground state of $HC_{14}H^+$ calculated with the DFT method at 2033 and 2013 cm^{-1}. The 609.8 nm band is the origin of the $\tilde{D}^2\Pi_g \leftarrow \tilde{X}^2\Pi_u$ system assigned for a reason similar to that in the case of $HC_{12}H^+$. The wavelengths of the bands observed in the spectra of $HC_{2n}H^+$ $n = 5-7$ with the suggested assignments are given in Table 1.

UV Transition of $HC_{2n}H^+$ $n = 4-7$. Besides the weak electronic transitions discussed above, the polyacetylene $HC_{2n}H^+$ $n = 4-7$ cations possess strong absorptions in the UV. They could not be detected in the case of HC_8H^+ and $HC_{10}H^+$ or identified for the larger polyacetylenes in the previous studies.[13] The reason was a poor matrix transmission in the UV range caused by the high kinetic energy of the deposited cations. For $HC_{12}H^+$ and $HC_{14}H^+$, they were observed before but not identified because they were concealed by absorptions of other species present in the matrix (e.g., $HC_{2n}H^-$). The electronic spectra of $HC_{2n}H^+$ $n = 4-7$ recorded presently in good optical quality matrixes reveal strong UV absorptions with intensities that correlate with the $\tilde{A}^2\Pi \leftarrow \tilde{X}^2\Pi$ system.

The UV section of the absorptions of the $HC_{2n}H^+$ $n = 4-7$ cations in a neon matrix is shown in Figure 3. The spectrum for each mass selection has been normalized to the same intensity of the strongest band, and their similar appearance is apparent. The spectrum is composed of two bands: the strong origin and a weaker one on the short-wavelength side. The origin peak has a multiplet structure, which becomes better resolved

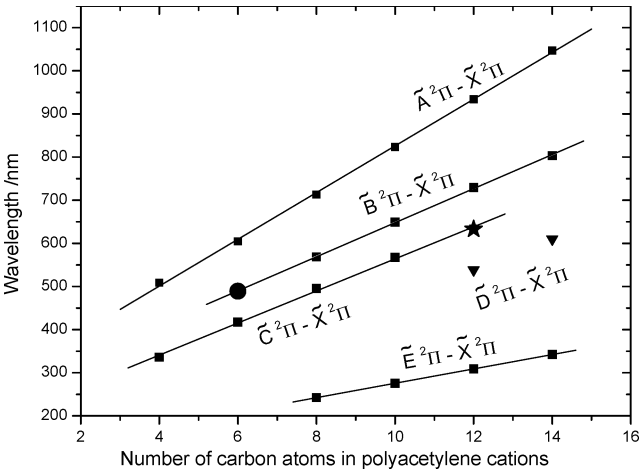

Figure 4. Wavelengths of the origin bands for the polyacetylene cations $HC_{2n}H^+$ ($n = 2-7$) in neon matrixes vs number of C atoms. Solid lines are linear least-square fits. The uppermost line is the known $\tilde{A}^2\Pi \leftarrow \tilde{X}^2\Pi$ transition;[13] remaining data are from the present studies. The star marks the wavelength of the ν_3 vibrational band in the $\tilde{B}^2\Pi_u$ state of $HC_{12}H^+$, which coincides with the origin of the $\tilde{C}^2\Pi_u \leftarrow \tilde{X}^2\Pi_g$ transition. The filled circle shows the $2\nu_3$ overtone of HC_6H^+ in the $\tilde{A}^2\Pi_g$ state, which lies where the origin of the $\tilde{B}^2\Pi_g \leftarrow \tilde{X}^2\Pi_u$ transition is expected.

passing from HC_8H^+ to $HC_{14}H^+$. The origin shifts monotonically to the red by ~33 nm increments. The weaker band is spaced from the origin by ~2000 cm^{-1}, which is the characteristic frequency of the C≡C stretching mode of polyacetylene chains. The absorption bands seen in Figure 2 are assigned to the $\tilde{E}^2\Pi \leftarrow \tilde{X}^2\Pi$ system of $HC_{2n}H^+$ $n = 4-7$ to be consistent with other observed transitions though the excited $\tilde{D}$ state was not observed for $n = 4$ and 5. The wavelengths with the suggested assignments are given in Table 1.

The integrated intensity of the UV bands of these cations has been compared with that for their $\tilde{A}^2\Pi \leftarrow \tilde{X}^2\Pi$ transition. The derived ratios (20% uncertainty) are 21, 29, 30, and 12 passing from HC_8H^+ to $HC_{14}H^+$, respectively. Hence, the oscillator strength of the $\tilde{E}^2\Pi \leftarrow \tilde{X}^2\Pi$ transition of $HC_{2n}H^+$ $n = 4-7$ is an order of magnitude larger than that for the $\tilde{A}^2\Pi \leftarrow \tilde{X}^2\Pi$ system, which has values in the $10^{-2}-10^{-1}$ range. Highly excited electronic states of HC_4H^+ have been studied by an ab initio CI method, which predicted a strong transition to the (4) $^2\Pi_u$ state near ~9 eV.[17] MRCI calculations have also been carried out for HC_6H^+;[18] however, they were restricted to the excited states, which lie only up to 6 eV above the ground state. One can estimate from the extrapolation of the observed trend for $HC_{2n}H^+$ $n = 4-7$ that a strong UV transition of HC_6H^+ is expected around 200 nm. However, this spectral range is not accessible in our experiment.

Transition Energy Dependence on the Size of $HC_{2n}H^+$. The wavelength of the origin band for the observed electronic transitions of $HC_{2n}H^+$ shifts monotonically. The linear dependence of the wavelength of the origin band versus number of carbon atoms is apparent. This relation is depicted in Figure 4. The top line corresponds to the known $\tilde{A}^2\Pi \leftarrow \tilde{X}^2\Pi$ transition,[13] whereas the remaining data come from the present studies.

The separation of the origin band of the $\tilde{A}^2\Pi \leftarrow \tilde{X}^2\Pi$ system and the onset of the new $\tilde{B}^2\Pi \leftarrow \tilde{X}^2\Pi$ transition decreases passing from larger to smaller cations, and in the case of HC_6H^+ falls in the region where vibrational bands of first transition are observed. The filled circle in the second fitted line shows the position where the origin band of the $\tilde{B}^2\Pi_g \leftarrow \tilde{X}^2\Pi_u$ transition of HC_6H^+ is expected. In the spectrum of HC_6H^+, a weak band around 489 nm is observed, and it was detected before in the gas phase and assigned to the $2\nu_3$ overtone of the $\tilde{A}^2\Pi_g \leftarrow \tilde{X}^2\Pi_u$ system.[5] It is an open question whether this band is the overtone or the origin of a new electronic transition because the energy (3840 cm^{-1}) is considerably higher than the twice fundamental mode of ν_3 (1880 cm^{-1}).

New weak transitions of polyacetylene cations form three series, where the lowest energy series starts with HC_8H^+ (or HC_6H^+), the second from HC_4H^+ but ends up with $HC_{10}H^+$, and the third (D) starts for $HC_{12}H^+$. The fitted lines of these series are nearly parallel. The asterisk in Figure 4 marks the position where the ν_3 vibrational band of $HC_{12}H^+$ was observed, which coincides with the origin band of the $\tilde{C}^2\Pi \leftarrow \tilde{X}^2\Pi$ transition. The reason that the transition to the $\tilde{C}$ electronic state of $HC_{12}H^+$ is not observed is not clear; perhaps it is too weak.

Polyacetylene cations possess many excited electronic states that are optically accessible from the ground state. The congestion of the excited electronic states in these systems causes their vibrational bands to overlap. Theoretical calculations on C_6^+ show the complexity arising in such open-shell systems by revealing several close-lying, mixed excited electronic states.[30,31]

In view of the number of new electronic transitions observed for the polyacetylene cations, it will be interesting to try to observe these in the gas phase using the ion trap approach used hitherto for their $\tilde{A}^2\Pi \leftarrow \tilde{X}^2\Pi$ transition.[14] There is also a need for a high-level theory for the excited electronic states in order to explain the details of present experimental data; configuration mixings appear significant. The calculations available for the smaller members of this homologous series do not provide this answer.

Acknowledgment. This study was supported by the Swiss National Science Foundation (project 200020 - 100019).

References and Notes

(1) Schüler, H.; Reinbeck, L. *Z. Naturforsch.* **1951**, *6a*, 160.
(2) Callomon, J. H. *Can. J. Phys.* **1956**, *34*, 1046.
(3) Allan, M.; Kloster-Jensen, E.; Maier, J. P. *Chem. Phys.* **1976**, *17*, 11.
(4) Kuhn, R.; Maier, J. P.; Ochsner, M. *Mol. Phys.* **1986**, *59*, 441.
(5) Klapstein, D.; Kuhn, R.; Maier, J. P.; Ochsner, M.; Zambach, W. *J. Phys. Chem.* **1984**, *88*, 5176.
(6) Lecoultre, J.; Maier, J. P.; Rösslein, M. *J. Chem. Phys.* **1988**, *89*, 6081.
(7) Smith, A. M.; Agreiter, J.; Härtle, M.; Engel, C.; Bondybey, V. M. *Chem. Phys.* **1994**, *189*, 315.
(8) Pfluger, D.; Sinclair, W. E.; Linnartz, H.; Maier, J. P. *Chem. Phys. Lett.* **1999**, *313*, 171.
(9) Pfluger, D.; Motylewski, T.; Linnartz, H.; Sinclair, W. E.; Maier, J. P. *Chem. Phys. Lett.* **2000**, *329*, 29.
(10) Cias, P.; Vaizert, O.; Denisov, A.; Mes, J.; Linnartz, H.; Maier, J. P. *J. Phys. Chem. A* **2002**, *106*, 9890.
(11) Sinclair, W. E.; Pfluger, D.; Linnartz, H.; Maier, J. P. *J. Chem. Phys.* **1999**, *110*, 296.
(12) Bondybey, V. E.; English, J. H. *J. Chem. Phys.* **1979**, *71*, 777.
(13) Freivogel, P.; Fulara, J.; Lessen, D.; Forney, D.; Maier, J. P. *Chem. Phys.* **1994**, *189*, 335.
(14) Dzhonson, A.; Jochnowitz, E. B.; Maier, J. P. *J. Phys. Chem. A* **2007**, *111*, 1887.
(15) Brogli, F.; Heilbronner, E.; Hornung, V.; Kloster-Jensen, E. *Helv. Chem. Acta.* **1973**, *56*, 2171.
(16) Allan, M.; Heilbronner, E.; Kloster-Jensen, E.; Maier, J. P. *Chem. Phys. Lett.* **1976**, *41*, 228.
(17) Bally, T.; Tang, W.; Jungen, M. *Chem. Phys. Lett.* **1992**, *190*, 453.
(18) Cao, Z.; Sigrid D. Peyerimhoff, S. D. *Phys. Chem. Chem. Phys.* **2001**, *3*, 1403.
(19) Komiha, N.; Rosmus, P.; Maier, J. P. *Mol. Phys.* **2006**, *104*, 3281.
(20) Freivogel, P.; Fulara, J.; Jakobi, M.; Forney, D.; Maier, J. P. *J. Chem. Phys.* **1995**, *103*, 54.
(21) Araki, M.; Linnartz, H.; Cias, P.; Denisov, A.; Fulara, J.; Batalov, A.; Shnitko, I.; Maier, J. P. *J. Chem. Phys.* **2003**, *118*, 10561.
(22) Araki, M.; Cias, P.; Denisov, A.; Fulara, J.; Maier, J. P. *Can. J. Chem.* **2004**, *82*, 1.

(23) Shnitko, I.; Fulara, J.; Batalov, A.; Gillery, C.; Masso, H.; Rosmus, P.; Maier, J. P. *J. Phys. Chem. A* **2006**, *110*, 2885.
(24) Batalov, A.; Fulara, J.; Shnitko, I.; Maier, J. P. *J. Phys. Chem. A* **2006**, *110*, 10404.
(25) Becke, A. D. *J. Chem. Phys.* **1993**, *98*, 564.
(26) Lee, C.; Yang, W.; Parr, R. G. *Phys. Rev. B* **1988**, *37*, 785.
(27) Kendall, R. A.; Dunning, T. H., Jr.; Harrison, R. J. *J. Chem. Phys.* **1992**, *96*, 6769.
(28) Sobolewski, A. L; Adamowicz, L. *J. Chem. Phys*. **1995**, *102*, 394.
(29) Grutter, M.; Wyss, M.; Fulara, J.; Maier, J. P. *J. Phys. Chem. A* **1998**, *102*, 9785.
(30) Gillery, C.; Rosmus, P.; Werner, H. F.; Stoll, H.; Maier, J. P. *Mol. Phys.* **2004**, *102*, 2227.
(31) Haubrich, J.; Mühlhäuser, M.; Peyerimhoff, S. D. *J. Mol. Spectrosc*. **2004**, *228*, 31.